Molecular imaging: The convergence of form and function

Christopher D. Malone, MD, and Isabel G. Newton, MD, PhD

Radiologic exams have become indispensable to the diagnostic process because they offer a non-invasive glimpse inside the human body. For many diseases, imaging facilitates diagnosis without the need for exploratory surgery or tissue sampling. Nonetheless, most radiologic exams are only capable of identifying the gross anatomic manifestations of the underlying microscopic derangements. As a result, radiologists are adept at identifying disease once it creates macroscopic structural changes, but they are less able to detect early or subtle changes or functional aberrations, as with pancreatic cancer, colon cancer and early diabetes.[1]

Without information regarding changes occurring at the cellular and molecular levels, the differential diagnoses of a given structural abnormality can be extensive. A 4-mm lung nodule or a subcentimeter liver mass can present challenges both for diagnosis and for patient management.[2] Also, traditional methods of monitoring disease can prove inadequate in the context of new and emerging treatments, where interval enlargement and contrast enhancement may not always indicate viable tumor. For instance, tumors treated with Y-90 radioembolization and drugs such as bevacizumab (Avastin®) can appear to enlarge or enhance due to edema, inflammation, or granulomatous tissue even in the absence of residual viable tumor.[3-6]

Recognition of these limitations has led to efforts to extract more information from structural imaging exams and closely correlate those findings with clinical implications. Studies have focused on correlating information derived from new magnetic resonance imaging (MRI) sequences with symptoms and pathologic findings.[7-9] Efforts to better align cross-sectional imaging findings with cancer outcomes have also led to improvements in RECIST (ie, Response Evaluation Criteria In Solid Tumors, a system of rules for assessing solid tumor response to treatment on imaging exams).[10-12] The most dramatic manifestations of this movement are the emerging fields of radiomics and radiogenomics, which concentrate on identifying quantitative imaging features that correlate with disease and gene expression.[13-16]

Molecular imaging (MI) and precision medicine

These advances portend an emerging paradigm shift from traditional anatomic imaging towards using radiologic exams to interrogate disease on genetic, molecular, and pathophysiological levels. This burgeoning field is called molecular imaging (MI), and cancer is its initial focus. Molecular imaging promises to deliver a more precise diagnosis based on a specific molecular disease process (eg, genetic mutation) rather than a phenotype (eg, lung mass). Such precision will guide optimal treatment selection and allow for better monitoring of disease progression

Dr. Newton is an Assistant Professor of Radiology at the University of California, San Diego, in San Diego, CA. Dr. Newton is also an Interventional Radiologist at the Veterans Affairs San Diego Healthcare System in San Diego, CA. Dr. Malone is an Interventional Radiology Fellow in the Department of Radiology of the University of Washington Medical Center in Seattle, WA.
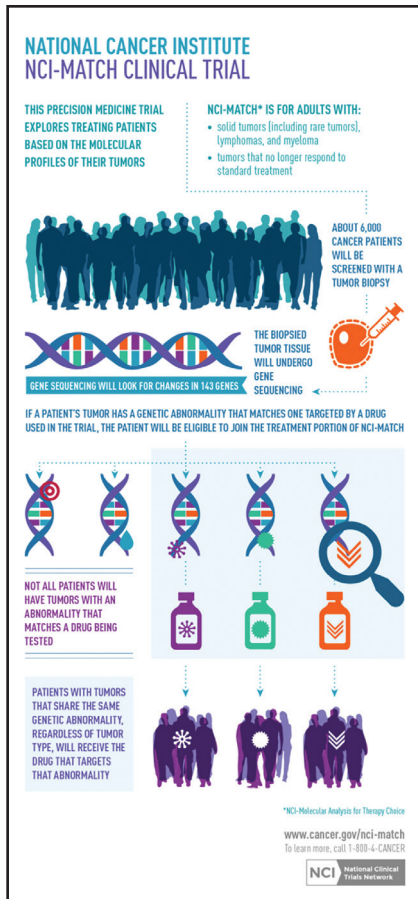
FIGURE 1. *The Precision Medicine Initiative through the National Cancer Institute sponsors a large trial (NCI-MATCH) to match targeted treatments to cancer patients based on their specific genetic alterations. Characterization of tumors with their molecular and genetic features through this initiative represents opportunities to develop complementary molecular imaging techniques. Infographic source: The National Cancer Institute.*

FIGURE 2. *Strategies for designing targeted MI agents compared to conventional untargeted agents. (A) Activatable MI agent. The inactive MI agent (black hexagon) has an inactive signal until it reaches the target and binds its tumor-specific ligand or receptor (orange diamond), allowing the signal to become active (blue hexagon). (B) Constitutively-active MI agent bound with inhibitor. The constitutively-active MI agent (blue hexagon) is bound to an inhibitor (green semicircle) until it reaches the target where an enzyme (scissors) in the microenvironment cleaves the bonds and releases the inhibitor, allowing the MI agent to bind to the tumor, where it is retained. (C) Constitutively-active MI agent decorated with tumor-specific antibodies. The constitutively-active MI agent (blue hexagon) is decorated with tumor-specific antibodies (blue Y's) that bind to tumor ligands (purple triangles) when it reaches the target. (D) Conventional untargeted contrast agent. Untargeted contrast agent (gray Gd circle) follows the blood pool and can accumulate in tumors passively across leaky tumor vasculature (dashed white line).*

and treatment response. This approach aims to limit patient exposure to unnecessary treatments and side effects. It could also check healthcare costs by minimizing therapeutic trial and error. Already underway are the preclinical molecular evaluation of brain gliomas for Epidermal Growth Factor Receptor (EGFR) signaling in cancer and the assessment of breast cancer tissue for HER2/neu, uPA receptor and hormone receptors.[17-22] This movement toward more personalized medicine is fueled by the Precision Medicine Initiative, also known as the *All of Us* Research Program, which sponsors a large trial
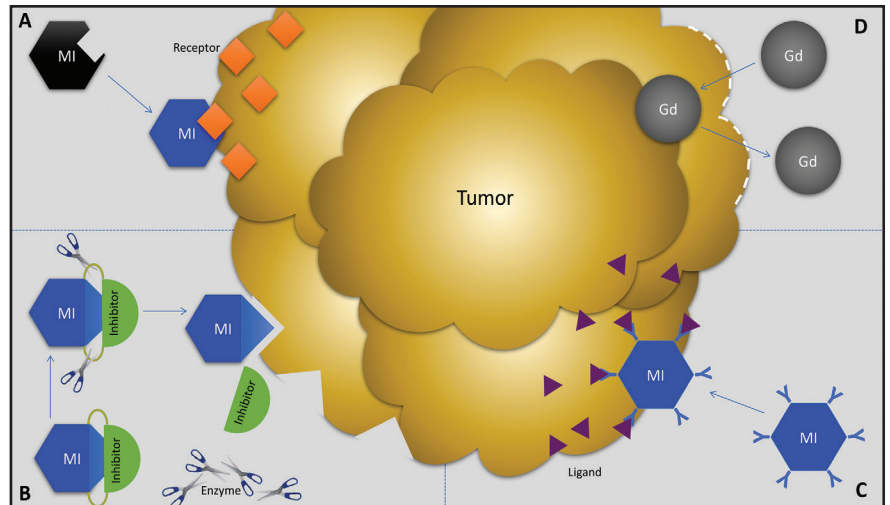
to match targeted treatments to cancer patients based on their specific genetic alterations (Figure 1).[23]

As MI emerges on the clinical scene, the role of the radiologist will be to provide an integrated assessment of tumor response that incorporates changes in size and enhancement with MI features. Interpretation will depend on familiarity with the particular molecular biomarkers of a given disease and their significance. Radiologists will learn the appearance of pathology using the new MI contrast agents, their enhancement kinetics, and their limitations within the context of structural imaging. Understanding available molecularly-targeted therapies and the role of MI examinations in predicting which patients will respond to these treatments will also enhance their value. Finally, a familiarity with the clinical trials of emerging targeted treatments, their imaging requirements, and the implications for surveillance and prognosis will help radiologists provide interpretations with greater clinical relevance.

Past strides towards MI

The initial pioneering in MI occurred predominantly in nuclear medicine (PET and SPECT) because of its sensitivity to picomolar amounts of radioactive substances and facility of incorporating radioactive elements into biologically relevant substances for imaging. Examples are Iodine-131 for thyroid function, [18F]FDG-PET to image glucose uptake as an indicator of hypermetabolic diseases including cancer, In[111]Ocreotide to image somatostatin receptors on neuroendocrine tumors and [18F]FLT to image thymidine kinase activity as an indicator of tumor cell proliferation.[24-35] These modalities are limited by low spatial and temporal resolution. The fusion of PET and SPECT with computed tomography (CT) or MRI helps, but it requires additional hardware and is subject to misregistration artifacts. Even so, nuclear medicine is ripe for the emergence of more innovations in MI.

Optical imaging is a form of MI that has found wide laboratory applications
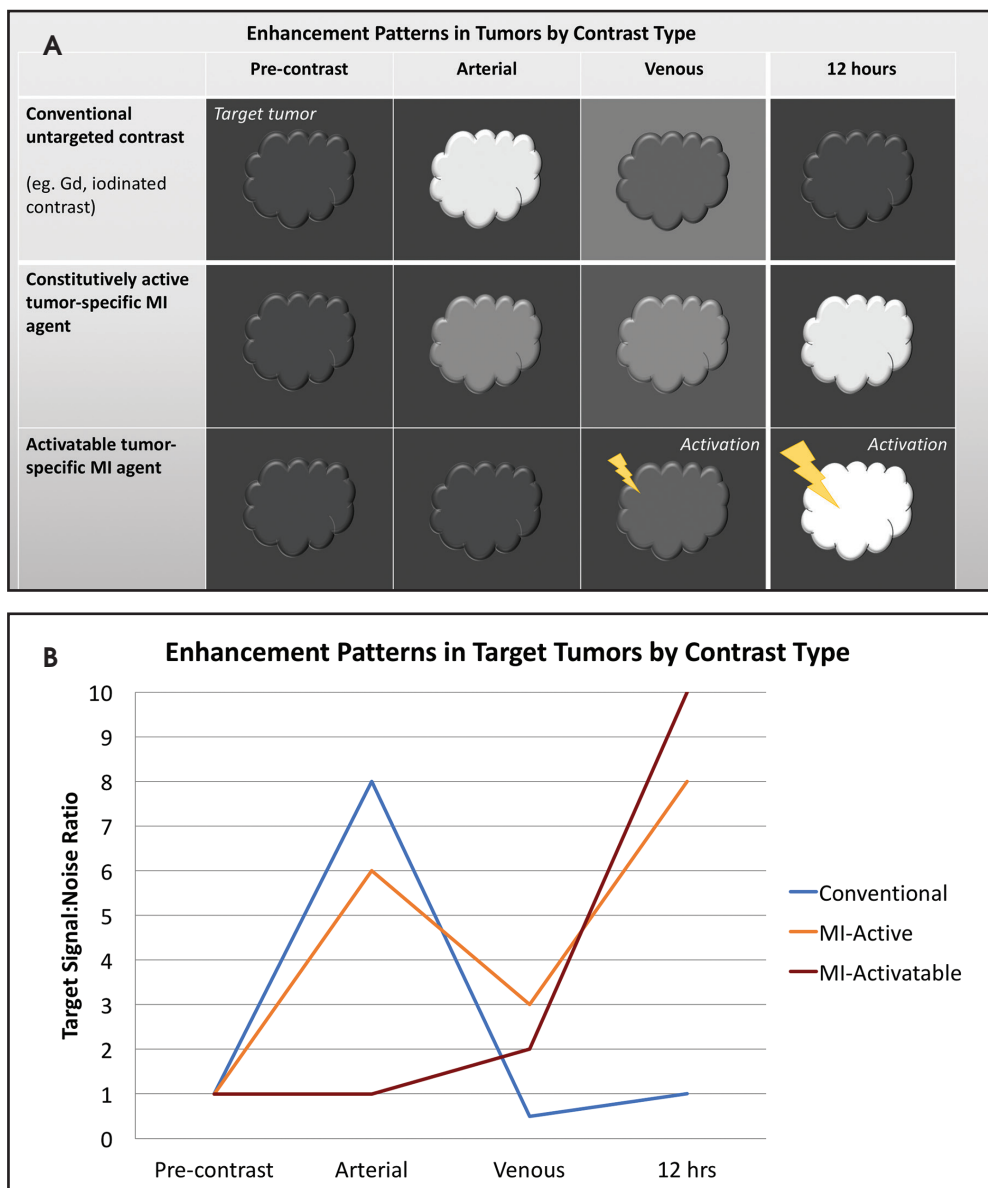
FIGURE 3. *Enhancement patterns in tumors by contrast type.*

(A) Schematic of the enhancement characteristics of a prototypical vascular tumor after intravenous administration of untargeted contrast (row 1) versus tumor-targeted MI agents (rows 2, 3) at four time points before (column 1) and after (columns 2, 3, 4) contrast administration. No tumor demonstrates enhancement pre-contrast (row 1). After untargeted contrast agent administration the tumor enhances brightly in the arterial phase and washes out in the venous phase relative to surrounding enhancement; by 12 hours later, the contrast has been cleared and neither the tumor nor surrounding tissue enhance. The constitutively-active MI agent behaves like a weak blood pool agent during the arterial phase. By the venous phase, the agent in the blood pool is washing out just as it begins to accumulate in the tumor, but background enhancement is also present. By 12 hours, the signal in the tumor is high relative to the background, which has washed out. By contrast, the activatable MI agent is only detectable once it interacts with the target (depicted by the lightning bolt), so enhancement is undetectable in the arterial phase and barely detectable by the venous phase. There is maximal tumor enhancement and no background enhancement at 12 hours.

(B) Illustrative graph of the enhancement characteristics of a prototypical vascular tumor after intravenous administration of untargeted contrast (blue) versus tumor-targeted MI agents (yellow, red) at four time points before and after contrast administration. All tumors demonstrate no enhancement precontrast, yielding a target signal-to-background noise ratio of 1. After untargeted contrast agent administration (blue), the tumor enhances brightly in the arterial phase, washes out in the venous phase relative to surrounding tissue; by 12 hours later, the contrast has been cleared and neither the tumor nor surrounding tissue enhance so the ratio is back to 1. The constitutively-active MI agent behaves like a weak blood pool agent during the arterial phase. By the venous phase, the agent is washing out just as it begins to accumulate in the tumor but background enhancement is also present. By 12 hours, the signal in the tumor is high relative to the background, which has washed out. By contrast, the activatable MI agent is only detectable once it interacts with the target so enhancement is undetectable in the arterial phase and barely detectable by the venous phase. There is maximal tumor enhancement and no background enhancement at 12 hours.

because it permits longitudinal in vivo visualization in both cells and small animals.[36,37] Unfortunately, there are few human applications because the energy emitted by fluorophores can penetrate only millimeters of tissue, at best. Optical imaging may be used by surgeons to identify tumor or nerves during open surgery.[38-41] However, there are no clinically relevant radiologic applications. This article will focus on the nascent field of MI agents for MRI, CT and ultrasound (US). The field faces daunting challenges, but driving this pursuit is the promise of revealing diseases based on more than gross anatomic appearance alone.

Towards smarter contrast agents

Molecular imaging agents have been termed "smart contrast agents," since they accumulate in specific targets or in the presence of a particular pathologic process (Figure 2A-C). Conventional iodinated contrast for CT and gadolinium (Gd) chelates for MRI are largely blood-pool agents with enhancement depending on tissue vascularity and integrity. Leaky vessels due to cancer, trauma, or inflammation permit passive accumulation of these agents (Figure 2D). A step smarter are hepatobiliary agents for MRI such as Eovist® (gadoxetate disodium; Bayer HealthCare Pharmaceuticals Inc, Whippany, NJ); because they are selectively taken up by hepatocytes, *negative* enhancement indicates the absence of normal hepatocytes and suggests the presence of disease.[42-44] Smart contrast agents selectively accumulate at their target and their signal can even be activatable (Figure 2A-C). As such, MI agents may become the in vivo imaging corollary to special stains or antibodies used histologically. This goal is fraught with challenges, including efficient delivery, avoidance of nontarget uptake, and adequate sensitivity, to name a few. Appreciating these challenges requires a basic understanding of the underlying molecular biology.

Nuts and bolts of MI

Radiologists familiar with the principles and language of molecular biology will lead the way in interpreting these emerging MI exams. Rapid advances in genetics have led to discoveries far beyond the basic understanding of DNA translation into RNA, which subsequently directs transcription into proteins. Cancer and other diseases can occur as a result of aberrations at any of these levels that manifest during synthesis or through post-synthetic modifications. DNA and proteins have received much attention, but research is focusing increasingly on RNA. There are various types of RNA, including messenger RNA (mRNA), transfer RNA (tRNA), and ribosomal RNA (rRNA), all of which mediate the process of translation.

An important noncoding form of RNA is microRNA (miRNA), which controls gene expression after transcription and plays a role in oncogenesis. In fact, the oncogene Myc and tumor suppressor gene p53 both act upon miRNAs.[45-49] Studies linking them to hepatocellular carcinoma (HCC) have resulted in the development of a system of molecular classification of HCC based on miRNA.[50,51] MicroRNAs have been shown to play a role in response to chemotherapy and in development of drug resistance.[52-54] They may serve as a cancer biomarker and could represent a target for disease monitoring and therapy or for combined imaging and therapy, termed *theranostics*.[55-60]

Proteins can have a variety of functions, including serving as ligands or modulators of signal transduction, receptors, or enzymes. Their amino acid composition and morphologic shape dictate their function. Because of the accessibility of proteins located on the cell surface or in the extracellular space, they represent common targets of MI agents.[61,62] Proteins are also used to make MI agents. Antibodies can make excellent MI agents due to their comparatively high binding specificity (Figure 2C). However, cost and loss of signal due to nonspecific uptake by organs of the reticuloendothelial system or proteins such as albumin potentially limit their utility.

An attractive candidate for MI agents are nanoparticles, a diverse group of molecules characterized by their 10-200 nm size and customizable shape and composition.[63,64] They can be made of a variety of materials, including lipids, polymers, iron oxide, gold, silica, carbon nanotubes, dendrimers, and semiconductors.[65-74] They can be decorated with ligands or receptors for targeting purposes.[75] Moreover, nanoparticles can be attached to high-payload concentrations for imaging purposes (eg, Gd or iron oxide for MRI) or therapeutic purposes (ie, drugs, genetic material, proteins).[76-78] Adding to their precision is the potential to engineer them to control the release of this payload over time.[79,80]

MI agent design

Fundamentals that guide MI agent design and utilization are how the agent reaches its target from the bloodstream, how it accumulates in the tissue, and how it is detected. Understanding these properties and their impact on the signal-to-noise ratio (SNR) is critical to interpreting patterns of enhancement. MI agents that travel within the bloodstream can behave like conventional untargeted agents within the first few minutes after administration; however, with time, they exit the blood stream to accumulate in tissues based on physical factors and biochemical interactions (Figure 3). Time points at least 6-12 hours post MI agent administration may offer the highest SNR.

Small molecules like nanoparticles can passively cross the blood brain barrier, cornea, and skin.[81,82] They can also traverse the leaky vasculature of tumors, which is termed the *enhanced permeability and retention effect* (EPR). EPR is even more pronounced with agents up to 400 nm and those with longer circulation times.[83] Tissues with a high concentration of phagocytes, such as those in the reticuloendothelial system, tend to accumulate MI agents like nanoparticles; if these tissues are not the target, then uptake contributes to background or noise.[84,85] Methods to mitigate this kind of nontarget uptake
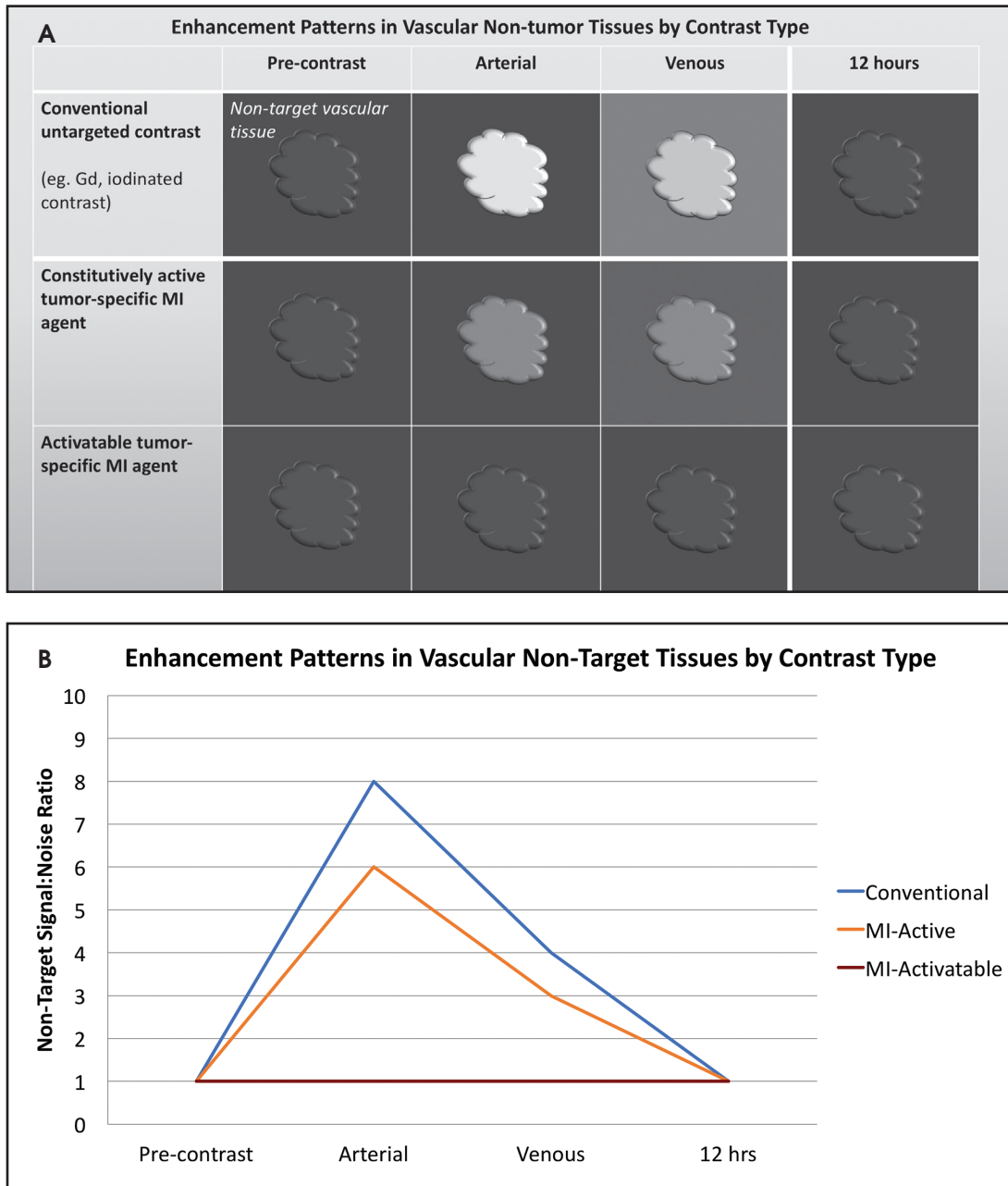
FIGURE 4. Enhancement patterns in vascular non-tumor tissues by contrast type.

(A) Schematic of the enhancement characteristics of a representative vascular non-tumor tissue after intravenous administration of conventional untargeted contrast (row 1) versus tumor-targeted MI agents (rows 2, 3) at four time points before (column 1) and after (columns 2, 3,4) contrast administration. All vascular non-tumor tissues demonstrate no enhancement pre-contrast (row 1). After conventional contrast agent administration, the vascular non-tumor tissue enhances brightly in the arterial phase, washes out in the venous phase and is cleared from the tissues by 12 hours. The constitutively active MI agent behaves like a weak blood pool agent during the arterial phase. By the venous phase, the agent is washing out of the vascular nontumor tissue but surrounding enhancement related to perfusion is also present. By 12 hours, the MI agent has washed out of all non-tumor tissues. By contrast, the activatable MI agent is only detectable once it interacts with the target. Since the tissue depicted represents non target tissue, there is no enhancement at any of the time points represented.

(B) Illustrative graph of the enhancement characteristics of vascular nontarget tissues after intravenous administration of untargeted contrast (blue) versus tumor-targeted MI agents (yellow, red) at four time points before and after contrast administration. All nontarget tissues demonstrate no enhancement pre-contrast, yielding a target signal-to-background noise ratio of 1. After untargeted contrast agent administration (blue), nontarget vascular tissue enhances brightly in the arterial phase and gradually washes out in delayed phases until it has been cleared 12 hours later. The constitutively-active MI agent behaves like a weak blood pool agent during the arterial phase and washes out on delayed points (yellow) similar to untargeted contrast agents (blue). Activatable MI agents are only detectable when interacting with their target, hence not displaying any nontarget tissue enhancement at any points.
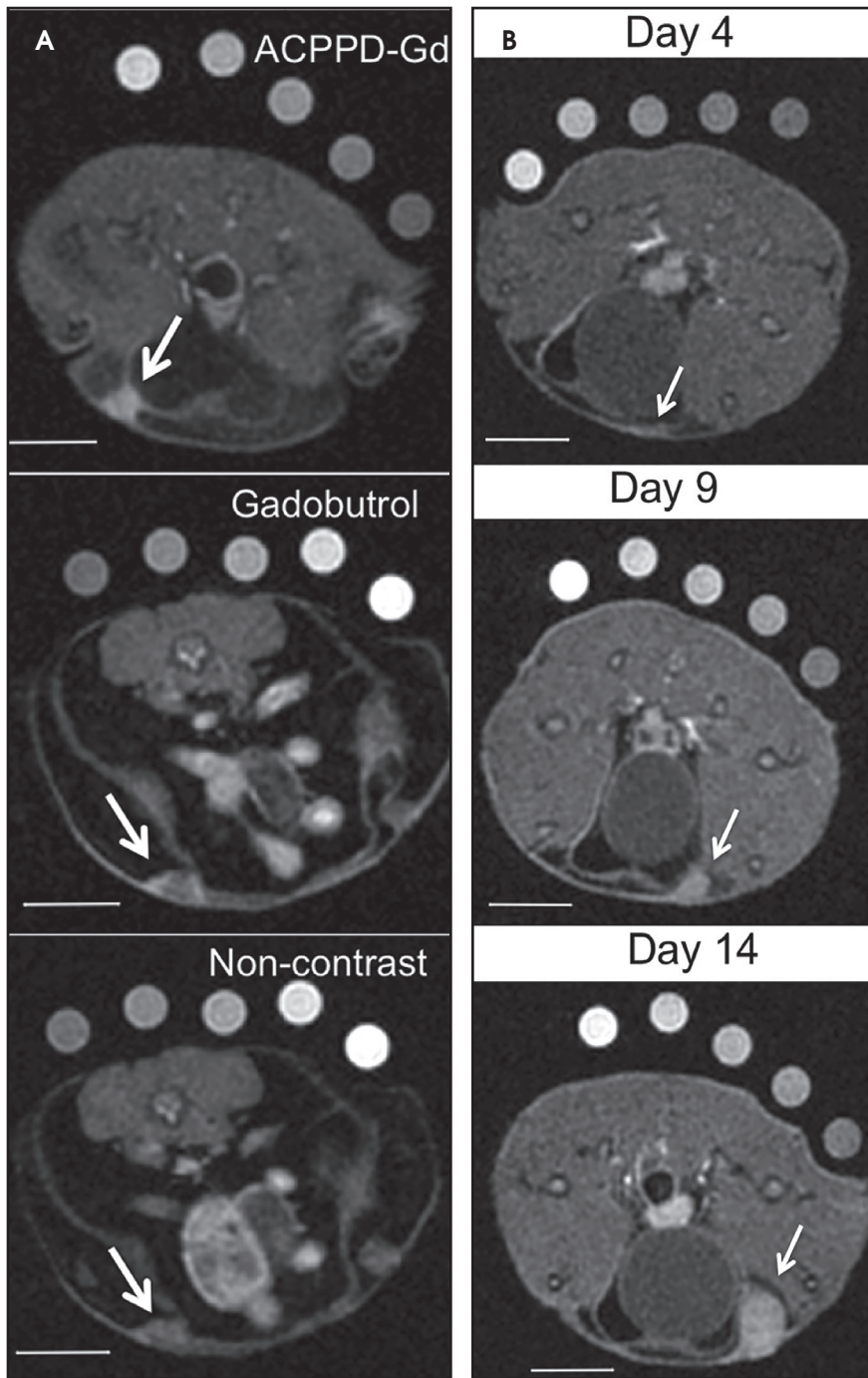
FIGURE 5. *Activatable cell penetrating peptide dendrimers conjugated to gadolinium (ACP-PD-Gd) are activated through MMP-cleavage and deposit in areas of high MMP expression, such as aggressive tumors. Mice harboring an aggressive mammary tumor line expressing high levels of MMP were imaged by T1-weighted MRI without contrast or after administration of either ACPPD-Gd or commercial Gadobutrol. (A) ACPPD-Gd administration results in more robust and conspicuous enhancement of small tumors less than 5 mm³ compared to those imaged after Gadobutrol or without contrast (white arrows); this effect is secondary to high accumulation of ACPPD-Gd from MMP cleavage. (B) Mice were imaged by MRI with ACP-PD-Gd at 4, 9, and 13 days after intramammary fat pad injection of a highly aggressive tumor line. At day 4, a small linear strip of enhancement appears which rapidly grows into a larger enhancing tumor at days 9 and 13 (white arrows). (Reproduced with permission from PLoS One.[74])*

are modifications such as PEGylation or direct delivery to the target.

Biochemical interactions with target molecules can enhance the retention of MI agents in target tissues while allowing them to wash out of nontarget tissues. These interactions can improve specificity and SNR. MI agents may be functionalized to interrogate protein expression by interacting with a specific receptor, enzyme, signal transduction regulator, or other ligand (Figure 2A-C). One example is the conjugation of an MRI contrast agent with a HER2 antibody for breast cancer imaging.[19] However, images derived from antibody-based MI agents are susceptible to noise if there is high nonspecific binding of the antibodies to "sticky" proteins.[86,87]

Once MI probes reach their target, optimizing signal strength and detectability presents another hurdle. The challenge is to accumulate enough probe in the target tissue so that it is visible compared to background. Each modality must overcome inherent limitations to achieve this goal but detectability ultimately depends on the amount and strength of the signal in a volume of tissue. There is a limit to how much detectable substance can be packed into a small volume, so an alternative is to augment the signal emitted by a few molecules, termed *signal amplification.*

Signal amplification can occur through the interaction of an MI agent with a target or in the presence of a specific environment. MRI probes can be designed to undergo conformational or relaxivity changes in certain microenvironments that enhance their visibility.[88,89] For example, the acidic conditions inside tumors can induce an MI probe to dissociate from the iron oxide quenching it, thereby unveiling its T1-shortening Gd molecule for MRI.[90,91] Another approach uses the chelate EgadMe to shield Gd from water until β-galactosidase cleaves and unveils it, enabling the Gd to interact with water and produce T1 shortening.[92,93]

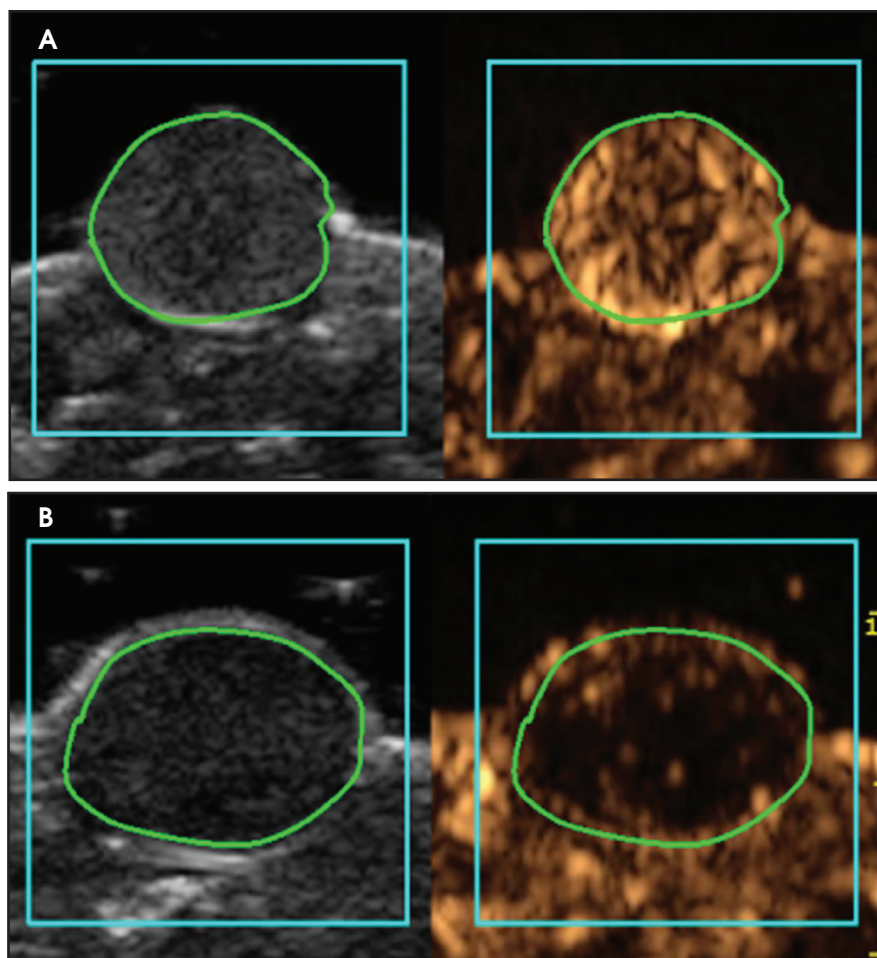Activatable MI agents represent a different strategy aimed at improving the SNR (Figures 3, 4). For these agents, a

FIGURE 6. *Microbubbles targeted to VEGFR-2 (BR55) can be used with ultrasound (US) to image VEGFR-2 expression in hepatocellular carcinoma (HCC) during Sorafenib treatment. Mice harboring HCC tumors were imaged 6 minutes after injection with BR55 at day 0 (A) and 14 (B) of Sorafenib treatment. (A) At day 0, high VEGFR-2 expression is evidenced by increased echogenicity on US due to high binding of BR55 microbubbles to the tumor. (B) After 14 days of Sorafenib, expression of VEGFR-2 has decreased secondary to treatment, resulting in minimal if any BR55 microbubble tumor binding and decreased signal on US. (Reproduced with permission from Springer Publishing and Molecular Imaging and Biology.*

receptor-ligand interaction or enzyme in the target releases a trapped signal or converts an inert molecule into a detectable one (Figure 2A,B). The fluorescent signal of an optical imaging agent is activated when cleaved by the matrix metalloproteinase (MMP) present in metastasizing tumors.[94] An enzyme can also induce the oligomerization of paramagnetic substrates to render an MRI agent visible.[95] In this sense, activatable MI agents can act as "switches" to monitor the molecular underpinnings of physiology and pathology. Others can also be activated externally with the application of energy in the form of US, light, or heat.[96,97]

This method permits regional anatomic control over MI agent activation.

Emerging MI agents by modality
Magnetic resonance imaging (MRI)

Magnetic resonance imaging achieves inherently superb soft tissue contrast, so molecular MRI stands to combine form and function in a powerful way. However, MRI faces the challenge of detecting MI agents that are usually in nanomolar concentrations, whereas the lower limits of sensitivity for Gd detection is in the micromolar range.[98] Current strategies aim to enhance the relaxivity of Gd to augment its signal.[99-101] Other

T1-based agents such as manganese (Mn) have also been employed.[102,103] T2-shortening agents primarily consist of iron oxide nanoparticles and have been clinically utilized to detect occult lymph node metastases in prostate cancer.[84] Non-proton MRI using fluorine (F-19) is a potentially attractive method for cell tracking in humans.[104-106] Other advanced MRI techniques with potential MI applications, such as chemical exchange saturation transfer (CEST), hyperpolarized MRI, and MR spectroscopy, are beyond the scope of this review but have been described previously.[107]

Several MI agents for MRI have been developed in preclinical settings and have a wide range of potential applications. Among the first were fibrin-targeted MI agents to detect thrombin, with applications for imaging cardiovascular disease.[108,109] Molecular imaging probes targeted to integrins could prove useful in MRI to detect angiogenesis and monitor anti-angiogenic cancer therapies.[110,111] Detection of surface phospholipids as a proxy for programmed cell death (ie, apoptosis) can also play a role in cancer and drug development.[112,113] Finally, MMPs have been frequent targets for MI agents because of their presence in aggressive and metastatic cancers (Figure 5).[41,73,74,114,115]

Computed tomography (CT)

Computed tomography is less suitable for MI since its sensitivity is at the millimolar scale, which is significantly lower than MRI (micromolar range), US (single microbubble), or nuclear medicine (picomolar range). Similar limitations apply to fluoroscopy. However, some work has been performed utilizing agents with strong photon attenuation properties, most notably gold nanoparticles, but also bismuth or iodine.[116-120] Multispectral CT imaging of macrophage burden in atherosclerotic plaques has been performed with gold-conjugated high density lipoprotein nanoparticles.[121] Given its low sensitivity and growing concerns over radiation exposure, CT is not likely to emerge as a favored modality for MI applications.

Ultrasound (US)

Molecular imaging with US uses targeted or functionalized microbubbles as contrast agents. Ultrasound detection of microbubbles relies on their non-linear response to low energy sound waves (Mechanical Index <0.3).[122,123] Microbubbles are generally composed of phospholipid shells encapsulating high molecular weight gases such as perfluorocarbons.[124] Contrast-enhanced US using agents such as Lumason® (Bracco Diagnostics Inc., Monroe Township, NJ) is most often performed clinically in echocardiography and for lesion characterization in the liver and kidney.[125-127] In the context of MI, microbubbles can be coated in the same fashion as MRI agents to target specific ligands of interest. Microbubbles targeted to bind to cell adhesion molecules (eg, V-CAM and I-CAM) and selectins have been used to assess atherosclerosis and angiogenesis, respectively.[128,129] Recently, a novel commercial microbubble agent BR55® (Bracco Suisse, Geneva, Switzerland) has been developed that specifically binds to vascular endothelial growth factor receptor-2 (VEGFR-2), which is the target of the antiangiogenic drug sorafenib (Nexavar®), used for HCC.[130,131] In preclinical experiments, BR55 can reveal VEGFR-2 expression in HCC after treatment with sorafenib, well before there are measurable changes in tumor size (Figure 6).[131-133] This agent has recently been clinically translated for use in patients with ovarian, breast, and prostate lesions.[134,135] High US energies can also be used to preferentially activate microbubbles and to disrupt endothelial linings to permit interrogation of areas beyond the vasculature.[136]

Limitations and challenges of MI

A major technical hurdle of MI, especially with MRI and CT, is sensitivity. Strategies for improving SNR, including signal amplification, activatable MI agents, and improved MI agent targeting, will help overcome this deficiency. Target selection also represents a critical challenge as the field moves forward. Diseases and their pathophysiology are diverse and markers have different significance for different diseases. Even so, the resources involved in developing an MI agent may be prohibitive if it is only meant to target one specific disease subtype. A solution is to find targets that can be broadly applied to a set of diseases but become specific in the appropriate context of disease. Candidate targets include MMP, thrombin, and EGFR. Partnerships with pathologists, molecular biologists, and other scientists can ensure that clinically and biologically relevant markers are chosen for development. Molecular imaging exams are also limited by the number of targets they can interrogate at once, whereas histology or flow cytometry can assess for numerous markers. A more complete disease picture could come from integration of MI with radiomics and big-data mining. Finally, MI agents could face stringent regulatory hurdles with variable approval from the U.S. Food and Drug Administration (FDA). Policy changes may have to evolve alongside this emerging technology. One option would be to develop FDA-approved protocols for generating customizable probes that can be made safely and affordably. Policies that facilitate rather than stifle innovations in MI will help propel the field towards more personalized medicine.

Conclusions

Since the first clinical use of x-rays, there have been stunning advances in the noninvasive visualization of anatomy and disease. In parallel, scientists have deepened their understanding of biology on the cellular, molecular and genetic levels. Molecular imaging hopes to capitalize on this knowledge and make key microscopic processes visible on clinical imaging exams. Radiologists are poised to usher in new MI techniques and enhance the value of their imaging interpretations. They will do so by understanding the molecular biology underlying these MI agents, including their potential applications and inherent challenges. The field is quickly evolving, so radiologists who partner with scientists, pathologists and other specialists will lead the way in developing and optimizing MI agents and their interpretation. Though the field faces significant hurdles, the promise of looking beyond structure to illuminate the functional underpinnings of disease makes it a challenge worth taking on.

REFERENCES

1. Pakzad F, Groves AM, Ell PJ. The role of positron emission tomography in the management of pancreatic cancer. *Semin Nucl Med*. 2006;36(3):248-256.
2. MacMahon H, Austin JH, Gamsu G, et al. Guidelines for management of small pulmonary nodules detected on CT scans: a statement from the Fleischner Society. *Radiology*. 2005;237(2):395-400.
3. Guo Y, Yaghmai V, Salem R, et al. Imaging tumor response following liver-directed intra-arterial therapy. *Abdom Imaging*. 2013;38(6):1286-1299.
4. Forner A, Ayuso C, Varela M, et al. Evaluation of tumor response after locoregional therapies in hepatocellular carcinoma: are response evaluation criteria in solid tumors reliable? *Cancer*. 2009;115(3):616-623.
5. Desar IM, van Herpen CM, van Laarhoven HW, et al. Beyond RECIST: molecular and functional imaging techniques for evaluation of response to targeted therapy. *Cancer Treat Rev*. 2009;35(4):309-321.
6. Hygino da Cruz LC, Jr., Rodriguez I, Doninguez RC, et al. Pseudoprogression and pseudoresponse: imaging challenges in the assessment of posttreatment glioma. *AJNR Am J Neuroradiol*. 2011;32(11):1978-1985.
7. White NS, McDonald CR, Farid N, et al. Improved conspicuity and delineation of high-grade primary and metastatic brain tumors using "restriction spectrum imaging": quantitative comparison with high B-value DWI and ADC. *AJNR Am J Neuroradiol*. 2013;34(5):958-964, S1.
8. Kothari PD, White NS, Farid N, et al. Longitudinal restriction spectrum imaging is resistant to pseudoresponse in patients with high-grade gliomas treated with bevacizumab. *AJNR Am J Neuroradiol*. 2013;34(9):1752-1757.
9. McCammack KC, Schenker-Ahmed NM, White NS, et al. Restriction spectrum imaging improves MRI-based prostate cancer detection. *Abdom Radiol (NY)*. 2016;41(5):946-953.
10. Grossmann P, Gutman DA, Dunn WD, Jr., et al. Imaging-genomics reveals driving pathways of MRI derived volumetric tumor phenotype features in Glioblastoma. *BMC Cancer*. 2016;16:611.
11. Marconi DG, Fregnani JH, Rossini RR, et al. Pre-treatment MRI minimum apparent diffusion coefficient value is a potential prognostic imaging biomarker in cervical cancer patients treated with definitive chemoradiation. *BMC Cancer*. 2016;16:556.
12. Huynh E, Coroller TP, Narayan V, et al. CT-based radiomic analysis of stereotactic body radiation therapy patients with lung cancer. *Radiother Oncol*. 2016;120(2):258-266.

13. Kotrotsou A, Zinn PO, Colen RR. Radiomics in brain tumors: an emerging technique for characterization of tumor environment. *Magn Reson Imaging Clin N Am*. 2016;24(4):719-729.

14. Banerjee S, Wang DS, Kim HJ, et al. A computed tomography radiogenomic biomarker predicts microvascular invasion and clinical outcomes in hepatocellular carcinoma. *Hepatology*. 2015;62(3):792-800.

15. Kerns SL, West CM, Andreassen CN, et al. Radiogenomics: the search for genetic predictors of radiotherapy response. *Future Oncol*. 2014;10(15):2391-2406.

16. Kickingereder P, Bonekamp D, Nowosielski M, et al. Radiogenomics of glioblastoma: machine learning-based classification of molecular characteristics by using multiparametric and multiregional MR imaging features. *Radiology*. 2016: 281(3):907-918.

17. Shazeeb MS, Sotak CH, DeLeo M, 3rd, et al. Targeted signal-amplifying enzymes enhance MRI of EGFR expression in an orthotopic model of human glioma. *Cancer Res*. 2011;71(6):2230-2239.

18. Artemov D, Mori N, Ravi R, et al. Magnetic resonance molecular imaging of the HER-2/neu receptor. *Cancer Res*. 2003;63(11):2723-2727.

19. Ding N, Sano K, Kanazaki K, et al. In vivo HER2-targeted magnetic resonance tumor imaging using iron oxide nanoparticles conjugated with Anti-HER2 fragment antibody. *Mol Imaging Biol*. 2016;18(6):870-876.

20. Yang L, Peng XH, Wang YA, et al. Receptor-targeted nanoparticles for in vivo imaging of breast cancer. *Clin Cancer Res*. 2009;15(14):4722-4732.

21. Pais A, Gunanathan C, Margalit R, et al. In vivo magnetic resonance imaging of the estrogen receptor in an orthotopic model of human breast cancer. *Cancer Res*. 2011;71(24):7387-7397.

22. Pereira PMR, Abma L, Henry KE, et al. Imaging of human epidermal growth factor receptors for patient selection and response monitoring - From PET imaging and beyond. *Cancer Lett. 2018:* 419;139-151.

23. Fox JL. Obama catapults patient-empowered precision medicine. *Nat Biotechnol*. 2015;33(4):325.

24. Seidlin SM, Marinelli LD, Oshry E. Radioactive iodine therapy; effect on functioning metastases of adenocarcinoma of the thyroid. *J Am Med Assoc*. 1946;132(14):838-847.

25. Zhu A, Lee D, Shim H. Metabolic positron emission tomography imaging in cancer detection and therapy response. *Semin Oncol*. 2011;38(1):55-69.

26. Blodgett TM, Meltzer CC, Townsend DW. PET/CT: form and function. *Radiology*. 2007;242(2):360-385.

27. Rohren EM, Turkington TG, Coleman RE. Clinical applications of PET in oncology. *Radiology*. 2004;231(2):305-332.

28. Zhuang H, Alavi A. 18-fluorodeoxyglucose positron emission tomographic imaging in the detection and monitoring of infection and inflammation. *Semin Nucl Med*. 2002;32(1):47-59.

29. Shreve PD, Anzai Y, Wahl RL. Pitfalls in oncologic diagnosis with FDG PET imaging: physiologic and benign variants. *Radiographics*. 1999;19(1):61-77; quiz 150-1.

30. Kjaer A, Dreyer M. Combined Indium-111 octreotide scintigraphy and low-dose computed tomography in localization of neuroendocrine tumors. *Clin Nucl Med*. 2003;28(6):506-508.

31. de Herder WW, Lamberts SW. Somatostatin and somatostatin analogues: diagnostic and therapeutic uses. *Curr Opin Oncol*. 2002;14(1):53-57.

32. Krenning EP, Kwekkeboom DJ, Bakker WH, et al. Somatostatin receptor scintigraphy with [111In-DTPA-D-Phe1]- and [123I-Tyr3]-octreotide: the Rotterdam experience with more than 1000 patients. *Eur J Nucl Med*. 1993;20(8):716-731.

33. Shields AF, Grierson JR, Dohmen BM, et al. Imaging proliferation in vivo with [F-18]FLT and positron emission tomography. *Nat Med*. 1998;4(11):1334-1336.

34. Vesselle H, Grierson J, Muzi M, et al. In vivo validation of 3'deoxy-3'-[(18)F]fluorothymidine ([(18)F]FLT) as a proliferation imaging tracer in humans: correlation of [(18)F]FLT uptake by positron emission tomography with Ki-67 immunohistochemistry and flow cytometry in human lung tumors. *Clin Cancer Res*. 2002;8(11):3315-3323.

35. Rendl G, Rettenbacher L, Holzmannhofer J, et al. Assessment of response to neoadjuvant radiochemotherapy with F-18 FLT and F-18 FDG PET/CT in patients with rectal cancer. *Ann Nucl Med*. 2015;29(3):284-294.

36. Pansare V, Hejazi S, Faenza W, et al. Review of Long-Wavelength Optical and NIR Imaging Materials: Contrast Agents, Fluorophores and Multifunctional Nano Carriers. *Chem Mater*. 2012;24(5):812-827.

37. Kosaka N, Ogawa M, Choyke PL, et al. Clinical implications of near-infrared fluorescence imaging in cancer. *Future Oncol*. 2009;5(9):1501-1511.

38. Nguyen QT, Tsien RY. Fluorescence-guided surgery with live molecular navigation--a new cutting edge. *Nat Rev Cancer*. 2013;13(9):653-662.

39. Orosco RK, Tsien RY, Nguyen QT. Fluorescence imaging in surgery. *IEEE Rev Biomed Eng*. 2013;6:178-187.

40. Whitney MA, Crisp JL, Nguyen LT, et al. Fluorescent peptides highlight peripheral nerves during surgery in mice. *Nat Biotechnol*. 2011;29(4):352-356.

41. Nguyen QT, Olson ES, Aguilera TA, et al. Surgery with molecular fluorescence imaging using activatable cell-penetrating peptides decreases residual cancer and improves survival. *Proc Natl Acad Sci U S A*. 2010;107(9):4317-4322.

42. Hamm B, Staks T, Muhler A, et al. Phase I clinical evaluation of Gd-EOB-DTPA as a hepatobiliary MR contrast agent: safety, pharmacokinetics, and MR imaging. *Radiology*. 1995;195(3):785-792.

43. Tsuboyama T, Onishi H, Kim T, et al. Hepatocellular carcinoma: hepatocyte-selective enhancement at gadoxetic acid-enhanced MR imaging--correlation with expression of sinusoidal and canalicular transporters and bile accumulation. *Radiology*. 2010;255(3):824-833.

44. Choi Y, Huh J, Woo DC, et al. Use of gadoxetate disodium for functional MRI based on its unique molecular mechanism. *Br J Radiol*. 2016;89(1058):20150666.

45. Bartel DP. MicroRNAs: target recognition and regulatory functions. *Cell*. 2009;136(2):215-233.

46. Ganju A, Khan S, Hafeez BB, et al. miRNA nanotherapeutics for cancer. *Drug Discov Today*. 2016 [Epub ahead of print].

47. Mayr C, Hemann MT, Bartel DP. Disrupting the pairing between let-7 and Hmga2 enhances oncogenic transformation. *Science*. 2007;315 (5818):1576-9.

48. Ding Y, Wang ZC, Zheng Y, et al. C-Myc functions as a competing endogenous RNA in acute promyelocytic leukemia. *Oncotarget*. 2016 7(35):56422-56430.

49. Chen L, Luo L, Chen W, et al. MicroRNA-24 increases hepatocellular carcinoma cell metastasis and invasion by targeting p53: miR-24 targeted p53. *Biomed Pharmacother*. 2016;84: 1113-1118.

50. Bronte F, Bronte G, Fanale D, et al. HepatomiRNoma: The proposal of a new network of targets for diagnosis, prognosis and therapy in hepatocellular carcinoma. *Crit Rev Oncol Hematol*. 2016;97:312-321.

51. Farra R, Grassi M, Grassi G, et al. Therapeutic potential of small interfering RNAs/micro interfering RNA in hepatocellular carcinoma. *World J Gastroenterol*. 2015;21(30):8994-9001.

52. Xu Y, Xia F, Ma L, et al. MicroRNA-122 sensitizes HCC cancer cells to adriamycin and vincristine through modulating expression of MDR and inducing cell cycle arrest. *Cancer Lett*. 2011;310(2):160-169.

53. Tsai WC, Hsu SD, Hsu CS, et al. MicroRNA-122 plays a critical role in liver homeostasis and hepatocarcinogenesis. *J Clin Invest*. 2012;122(8): 2884-2897.

54. Xu G, Zhang Y, Wei J, et al. MicroRNA-21 promotes hepatocellular carcinoma HepG2 cell proliferation through repression of mitogen-activated protein kinase-kinase 3. *BMC Cancer*. 2013;13:469.

55. Mullick Chowdhury S, Wang TY, Bachawal S, et al. Ultrasound-guided therapeutic modulation of hepatocellular carcinoma using complementary microRNAs. *J Control Release*. 2016;238: 272-280.

56. Allegra A, Alonci A, Campo S, et al. Circulating microRNAs: new biomarkers in diagnosis, prognosis and treatment of cancer (review). *Int J Oncol*. 2012;41(6):1897-1912.

57. Rapisuwon S, Vietsch EE, Wellstein A. Circulating biomarkers to monitor cancer progression and treatment. *Comput Struct Biotechnol J*. 2016;14:211-222.

58. Boye A, Yang Y. Hepatic microRNA orchestra: a new diagnostic, prognostic and theranostic tool for hepatocarcinogenesis. *Mini Rev Med Chem*. 2014;14(10):837-852.

59. Bertoli G, Cava C, Castiglioni I. MicroRNAs: new biomarkers for diagnosis, prognosis, therapy prediction and therapeutic tools for breast cancer. *Theranostics*. 2015;5(10):1122-1143.

60. Matin F, Jeet V, Clements JA, et al. MicroRNA theranostics in prostate cancer precision medicine. *Clin Chem*. 2016;62(10):1318-1333.

61. Rosenberger I, Strauss A, Dobiasch S, et al. Targeted diagnostic magnetic nanoparticles for medical imaging of pancreatic cancer. *J Control Release*. 2015;214:76-84.

62. Winnard P, Jr., Raman V. Real time non-invasive imaging of receptor-ligand interactions in vivo. *J Cell Biochem*. 2003;90(3):454-463.

63. Ferrari M. Cancer nanotechnology: opportunities and challenges. *Nat Rev Cancer*. 2005;5(3):1 61-171.

64. Sullivan DC, Ferrari M. Nanotechnology and tumor imaging: seizing an opportunity. *Mol Imaging*. 2004;3(4):364-369.

65. Sapra P, Tyagi P, Allen TM. Ligand-targeted liposomes for cancer treatment. *Curr Drug Deliv*. 2005;2(4):369-3681.

66. Perez JM, Josephson L, Weissleder R. Use of magnetic nanoparticles as nanosensors to probe for molecular interactions. *Chembiochem*. 2004;5(3):261-264.

67. Mallidi S, Larson T, Tam J, et al. Multiwavelength photoacoustic imaging and plasmon resonance coupling of gold nanoparticles for selective detection of cancer. *Nano Lett*. 2009;9(8):2825-2831.

68. Ke H, Wang J, Dai Z, et al. Gold-nanoshelled microcapsules: a theranostic agent for ultrasound contrast imaging and photothermal therapy. *Angew Chem Int Ed Engl*. 2011;50(13):3017-3021.

69. Huang P, Bao L, Zhang C, et al. Folic acid-conjugated silica-modified gold nanorods for X-ray/CT imaging-guided dual-mode radiation and photo-thermal therapy. *Biomaterials*. 2011;32(36):9796-9809.

70. Yao G, Wang L, Wu Y, et al. FloDots: luminescent nanoparticles. *Anal Bioanal Chem*. 2006;385(3):518-524.

71. Liu Z, Davis C, Cai W, et al. Circulation and long-term fate of functionalized, biocompatible single-walled carbon nanotubes in mice probed by Raman spectroscopy. *Proc Natl Acad Sci U S A*. 2008;105(5):1410-1415.

72. Prato M, Kostarelos K, Bianco A. Functionalized carbon nanotubes in drug design and discovery. *Acc Chem Res*. 2008;41(1):60-68.

73. Olson ES, Jiang T, Aguilera TA, et al. Activatable cell penetrating peptides linked to nanoparticles as dual probes for in vivo fluorescence and MR imaging of proteases. *Proc Natl Acad Sci U S A*. 2010;107(9):4311-4316.

74. Malone CD, Olson ES, Mattrey RF, et al. Tumor detection at 3 Tesla with an activatable cell penetrating peptide dendrimer (ACPPD-Gd), a T1 magnetic resonance (MR) molecular imaging agent. *PLoS One*. 2015;10(9):e0137104.

75. Nap RJ, Szleifer I. How to optimize binding of coated nanoparticles: coupling of physical interactions, molecular organization and chemical state. *Biomater Sci*. 2013;1(8):814-823.

76. Thakor AS, Gambhir SS. Nanooncology: the future of cancer diagnosis and therapy. *CA Cancer J Clin*. 2013;63(6):395-418.

77. Shen Z, Wu A, Chen X. Iron oxide nanoparticle based contrast agents for magnetic resonance imaging. *Mol Pharm*. 2016 [Epub ahead of print].

78. Li L, Tong R, Li M, et al. Self-assembled gemcitabine-gadolinium nanoparticles for magnetic resonance imaging and cancer therapy. *Acta Biomater*. 2016;33:34-39.

79. Roy I, Mitra S, Maitra A, et al. Calcium phosphate nanoparticles as novel non-viral vectors for targeted gene delivery. *Int J Pharm*. 2003;250(1):25-33.

80. Wang H, Wang S, Liao Z, et al. Folate-targeting magnetic core-shell nanocarriers for selective drug release and imaging. *Int J Pharm*. 2012;430(1-2):342-349.

81. Chakraborty M, Jain S, Rani V. Nanotechnology: emerging tool for diagnostics and therapeutics. *Appl Biochem Biotechnol*. 2011;165(5-6):1178-1187.

82. Gao H. Progress and perspectives on targeting nanoparticles for brain drug delivery. *Acta Pharm Sin B*. 2016;6(4):268-286.

83. Matsumura Y, Maeda H. A new concept for macromolecular therapeutics in cancer chemotherapy: mechanism of tumoritropic accumulation of proteins and the antitumor agent smancs. *Cancer Res*. 1986;46(12 Pt 1):6387-6392.

84. Harisinghani MG, Barentsz J, Hahn PF, et al. Noninvasive detection of clinically occult lymph-node metastases in prostate cancer. *N Engl J Med*. 2003;348(25):2491-2499.

85. Weissleder R, Elizondo G, Wittenberg J, et al. Ultrasmall superparamagnetic iron oxide: characterization of a new class of contrast agents for MR imaging. *Radiology*. 1990;175(2):489-493.

86. Ni Y, Bormans G, Chen F, et al. Necrosis avid contrast agents: functional similarity versus structural diversity. *Invest Radiol*. 2005;40(8):526-535.

87. Olson ES, Aguilera TA, Jiang T, et al. In vivo characterization of activatable cell penetrating peptides for targeting protease activity in cancer. *Integr Biol (Camb)*. 2009;1(5-6):382-393.

88. van Elk M, Murphy BP, Eufrasio-da-Silva T, et al. Nanomedicines for advanced cancer treatments: Transitioning towards responsive systems. *Int J Pharm*. 2016;515(1-2):132-164.

89. Querol M, Bogdanov A, Jr. Environment-sensitive and enzyme-sensitive MR contrast agents. *Handb Exp Pharmacol*. 2008(185 Pt 2):37-57.

90. Viger ML, Sankaranarayanan J, de Gracia Lux C, et al. Collective activation of MRI agents via encapsulation and disease-triggered release. *J Am Chem Soc*. 2013;135(21):7847-7850.

91. Santra S, Jativa SD, Kaittanis C, et al. Gadolinium-encapsulating iron oxide nanoprobe as activatable NMR/MRI contrast agent. *ACS Nano*. 2012;6(8):7281-7294.

92. Louie AY, Huber MM, Ahrens ET, et al. In vivo visualization of gene expression using magnetic resonance imaging. *Nat Biotechnol*. 2000;18(3):321-325.

93. Cosentino U, Pitea D, Moro G, et al. Conformational behaviour determines the low-relaxivity state of a conditional MRI contrast agent. *Phys Chem Chem Phys*. 2009;11(20):3943-3950.

94. Savariar EN, Felsen CN, Nashi N, et al. Real-time in vivo molecular detection of primary tumors and metastases with ratiometric activatable cell-penetrating peptides. *Cancer Res*. 2013;73(2):855-864.

95. Bogdanov A, Jr., Matuszewski L, Bremer C, et al. Oligomerization of paramagnetic substrates result in signal amplification and can be used for MR imaging of molecular targets. *Mol Imaging*. 2002;1(1):16-23.

96. Tong R, Chiang HH, Kohane DS. Photoswitchable nanoparticles for in vivo cancer chemotherapy. *Proc Natl Acad Sci U S A*. 2013;110(47):19048-19053.

97. Zhu F, Jiang Y, Luo F, et al. Effectiveness of localized ultrasound-targeted microbubble destruction with doxorubicin liposomes in H22 mouse hepatocellular carcinoma model. *J Drug Target*. 2015;23(4):323-334.

98. Massoud TF, Gambhir SS. Molecular imaging in living subjects: seeing fundamental biological processes in a new light. *Genes Dev*. 2003;17(5):545-580.

99. Clavijo Jordan MV, Beeman SC, Baldelomar EJ, et al. Disruptive chemical doping in a ferritin-based iron oxide nanoparticle to decrease r2 and enhance detection with T1-weighted MRI. *Contrast Media Mol Imaging*. 2014;9(5):323-332.

100. Ghaghada KB, Ravoori M, Sabapathy D, et al. New dual mode gadolinium nanoparticle contrast agent for magnetic resonance imaging. *PLoS One*. 2009;4(10):e7628.

101. Tchouala Nofiele J, Cheng W, Haedicke IE, et al. Ultrashort echo time magnetic resonance imaging of the lung using a high-relaxivity t1 blood-pool contrast agent. *Mol Imaging*. 2014;13.

102. Hsu BY, Ng M, Tan A, et al. pH-Activatable MnO-Based fluorescence and magnetic resonance bimodal nanoprobe for cancer imaging. *Adv Healthc Mater*. 2016;5(6):721-729.

103. Yu M, Beyers RJ, Gorden JD, et al. A magnetic resonance imaging contrast agent capable of detecting hydrogen peroxide. *Inorg Chem*. 2012;51(17):9153-9155.

104. Janjic JM, Ahrens ET. Fluorine-containing nanoemulsions for MRI cell tracking. *Wiley Interdiscip Rev Nanomed Nanobiotechnol*. 2009;1(5):492-501.

105. Ahrens ET, Helfer BM, O'Hanlon CF, et al. Clinical cell therapy imaging using a perfluorocarbon tracer and fluorine-19 MRI. *Magn Reson Med*. 2014;72(6):1696-1701.

106. Fink C, Gaudet JM, Fox MS, et al. [19]F- perfluorocarbon-labeled human peripheral blood mononuclear cells can be detected in vivo using clinical MRI parameters in a therapeutic cell setting. *Sci Rep*. 2018:8(1);590.

107. Haris M, Yadav SK, Rizwan A, et al. Molecular magnetic resonance imaging in cancer. *J Transl Med*. 2015;13:313.

108. Winter PM, Caruthers SD, Yu X, et al. Improved molecular imaging contrast agent for detection of human thrombus. *Magn Reson Med*. 2003;50(2):411-416.

109. Botnar RM, Perez AS, Witte S, et al. In vivo molecular imaging of acute and subacute thrombosis using a fibrin-binding magnetic resonance imaging contrast agent. *Circulation*. 2004;109(16):2023-2029.

110. Waters EA, Chen J, Yang X, et al. Detection of targeted perfluorocarbon nanoparticle binding using 19F diffusion weighted MR spectroscopy. *Magn Reson Med*. 2008;60(5):1 232-1236.

111. Kazmierczak PM, Schneider M, Habereder T, et al. Alphavss3-integrin-targeted magnetic resonance imaging for the assessment of early antiangiogenic therapy effects in orthotopic breast cancer xenografts. *Invest Radiol*. 2016;51(11):746-755.

112. Burtea C, Laurent S, Lancelot E, et al. Peptidic targeting of phosphatidylserine for the MRI detection of apoptosis in atherosclerotic plaques. *Mol Pharm*. 2009;6(6):1903-1919.

113. van Tilborg GA, Vucic E, Strijkers GJ, et al. Annexin A5-functionalized bimodal nanoparticles for MRI and fluorescence imaging of atherosclerotic plaques. *Bioconjug Chem*. 2010;21(10): 1794-1803.

114. Ansari C, Tikhomirov GA, Hong SH, et al. Development of novel tumor-targeted theranostic nanoparticles activated by membrane-type matrix metalloproteinases for combined cancer magnetic resonance imaging and therapy. *Small*. 2014;10(3):566-575, 417.

115. Isaacson KJ, Martin Jensen M, Subrahmanyam NB, et al. Matrix-metalloproteinases as targets for controlled delivery in cancer: An analysis of upregulation and expression. *J Control Release*. 2017: 259;62-75.

116. Rabin O, Manuel Perez J, Grimm J, et al. An X-ray computed tomography imaging agent based on long-circulating bismuth sulphide nanoparticles. *Nat Mater*. 2006;5(2):118-122.

117. Chen J, Yang XQ, Qin MY, et al. Hybrid nanoprobes of bismuth sulfide nanoparticles and CdSe/ZnS quantum dots for mouse computed tomography/fluorescence dual mode imaging. *J Nanobiotechnology*. 2015;13:76.

118. Lee N, Choi SH, Hyeon T. Nano-sized CT contrast agents. *Adv Mater*. 2013;25(19):2641-2660.

119. Hallouard F, Briancon S, Anton N, et al. Poly(ethylene glycol)-poly(epsilon-caprolactone) iodinated nanocapsules as contrast agents for X-ray imaging. *Pharm Res*. 2013;30(8):2023-2035.

120. Hyafil F, Cornily JC, Feig JE, et al. Noninvasive detection of macrophages using a nanoparticulate contrast agent for computed tomography. *Nat Med*. 2007;13(5):636-341.

121. Cormode DP, Roessl E, Thran A, et al. Atherosclerotic plaque composition: analysis with multicolor CT and targeted gold nanoparticles. *Radiology*. 2010;256(3):774-782.

122. Phillips P, Gardner E. Contrast-agent detection and quantification. *Eur Radiol*. 2004;14 Suppl 8:P4-10.

123. Klibanov AL, Rasche PT, Hughes MS, et al. Detection of individual microbubbles of an ultrasound contrast agent: fundamental and pulse inversion imaging. *Acad Radiol*. 2002;9 Suppl 2:S279-281.

124. Deshpande N, Needles A, Willmann JK. Molecular ultrasound imaging: current status and future directions. *Clin Radiol*. 2010;65(7):567-581.

125. Schneider M. Characteristics of SonoVue-rade mark. *Echocardiography*. 1999;16(7, Pt 2):743-746.

126. Claudon M, Dietrich CF, Choi BI, et al. Guidelines and good clinical practice recommendations for Contrast Enhanced Ultrasound (CEUS) in the liver - update 2012: A WFUMB-EFSUMB initiative in cooperation with representatives of AFSUMB, AIUM, ASUM, FLAUS and ICUS. *Ultrasound Med Biol*. 2013;39(2):187-210.

127. Sun D, Wei C, Li Y, et al. Contrast-enhanced ultrasonography with quantitative analysis allows differentiation of renal tumor histotypes. *Sci Rep*. 2016;6:35081.

128. Spivak I, Rix A, Schmitz G, et al. Low-Dose Molecular Ultrasound Imaging with E-Selectin-Targeted PBCA Microbubbles. *Mol Imaging Biol*. 2016;18(2):180-190.

129. Wu J, Leong-Poi H, Bin J, et al. Efficacy of contrast-enhanced US and magnetic microbubbles targeted to vascular cell adhesion molecule-1 for molecular imaging of atherosclerosis. *Radiology*. 2011;260(2):463-471.

130. Llovet JM, Ricci S, Mazzaferro V, et al. Sorafenib in advanced hepatocellular carcinoma. *N Engl J Med*. 2008;359(4):378-390.

131. Sugimoto K, Moriyasu F, Negishi Y, et al. Quantification in molecular ultrasound imaging: a comparative study in mice between healthy liver and a human hepatocellular carcinoma xenograft. *J Ultrasound Med*. 2012;31(12):1909-1916.

132. Hu Q, Wang XY, Kang LK, et al. RGD-Targeted ultrasound contrast agent for longitudinal assessment of Hep-2 tumor angiogenesis in vivo. *PLoS One*. 2016;11(2):e0149075.

133. Baron Toaldo M, Salvatore V, Marinelli S, et al. Use of VEGFR-2 targeted ultrasound contrast agent for the early evaluation of response to sorafenib in a mouse model of hepatocellular carcinoma. *Mol Imaging Biol*. 2015;17(1):29-37.

134. Willmann JK, Bonomo L, Testa CA, et al. Ultrasound molecular imaging with BR55 in patients with breast and ovarian lesions: first-in-human results. *J Clin Oncol*. 2017: 35(19); 2133-2140.

135. Smeenge M, Tranquart F, Mannaerts CK, et al. First-in-human ultrasound molecular imaging with a VEGFR2-specific ultrasound molecular contrast agent (BR55) in prostate cancer: A safety and feasibility pilot study. *Invest Radiol*. 2017: 52(7):419-427.

136. Borden MA, Sarantos MR, Stieger SM, et al. Ultrasound radiation force modulates ligand availability on targeted contrast agents. *Mol Imaging*. 2006;5(3):139-147.